



## Sensitivity of GOCE gradients on Greenland mass variation and changes in ice topography

Herceg, Matija; Tscherning, Carl Christian; Fredenslund Levinsen, Joanna

*Published in:*  
Journal of Geodetic Science

*Link to article, DOI:*  
[10.2478/jogs-2014-0001](https://doi.org/10.2478/jogs-2014-0001)

*Publication date:*  
2014

*Document Version*  
Publisher's PDF, also known as Version of record

[Link back to DTU Orbit](#)

*Citation (APA):*  
Herceg, M., Tscherning, C. C., & Fredenslund Levinsen, J. (2014). Sensitivity of GOCE gradients on Greenland mass variation and changes in ice topography. *Journal of Geodetic Science*, 4(1), 8-18.  
<https://doi.org/10.2478/jogs-2014-0001>

---

### General rights

Copyright and moral rights for the publications made accessible in the public portal are retained by the authors and/or other copyright owners and it is a condition of accessing publications that users recognise and abide by the legal requirements associated with these rights.

- Users may download and print one copy of any publication from the public portal for the purpose of private study or research.
- You may not further distribute the material or use it for any profit-making activity or commercial gain
- You may freely distribute the URL identifying the publication in the public portal

If you believe that this document breaches copyright please contact us providing details, and we will remove access to the work immediately and investigate your claim.

## Research Article

## Open Access

M. Herceg\*, C. C. Tscherning, and J. F. Levinsen

# Sensitivity of Goce gradients on Greenland mass variation and changes in ice topography

**Abstract:** The Gravity field and steady state Ocean Circulation Explorer (GOCE) maps variations in the gravity field by observing second order derivatives (gradients) of the Earth gravitational potential. Flying in the low altitude of 255 km and having a spatially dense data distribution of short wavelengths of the gravity field, GOCE may be used to enhance the time varying gravity signal coming from the GRACE satellites.

The GOCE gradients may potentially be used for the determination of residual masses in local regions. This can be done using Least-Squares Collocation (LSC) or the Reduced Point Mass (RPM) method. In this study, different gravity field solutions are calculated by the use of RPM, LSC and GOCE gradients, respectively. Gravity field time series are created and presented for the six consecutive months of GOCE gradient observations, data being acquired between November 2009 and June 2010. Corresponding gravity anomaly results are used for the calculation of ice mass changes by the use of the RPM method. The results are then compared with the computed topographic effect of the ice by the use of a modified topographic correction and the *Gravsoft TC* program.

The maximal gravity changes at the ground predicted from GOCE gradients are between 2 and 4 mGal for the period considered. The gravity anomaly estimation error arising from the GOCE gradient data using only  $T_{zz}$  with an associated error of 20 mE is 11 mGal. This analysis shows the potential of using GOCE data for observations of ice mass changes although the GOCE dataset is limited to only six months. We expect four years of GOCE gradient observations to be available by mid-2014. This will increase the accuracy and spatial resolution of the GOCE measurements, which may lead to an accuracy necessary for observing ice mass changes.

**Keywords:** collocation, gradients, mass change, reduced point mass

\*Corresponding Author: M. Herceg: E-mail: matija.herceg@geo.ku.dk

## 1 Introduction

The Gravity field and steady state Ocean Circulation Explorer (GOCE) is the most advanced gravity space mission to date, and since 2009 it has mapped global variations in the gravity field with remarkable detail and accuracy. The success of the GOCE mission depends on adequate methodologies being developed for extracting the gravity field from its observations and for combining the gravity field with information from other sources. In such a way, GOCE derived data has a possibility to add the insight needed in order to further our understanding of the physical processes occurring inside the Earth and on its surface. This can be done through a broad range of application, e.g. in the fields of geodesy, solid Earth physics, oceanography and cryospheric research.

In order to get a better picture of the effect of the present-day climate changes in polar regions, research has been carried out focusing on the regions where changes in the Greenland ice sheet have been observed, e.g. Krabill et al. (2004), Velicogna and Wahr (2005), Joughin et al. (2010). Most of the largest outlet glaciers have experienced accelerated retreats, causing an increased ice discharge (Sørensen, 2010). The largest accelerations have been observed by the Helheim glacier, Kangerdlugssuaq and Jakobshavn Isbræ (JI) (Howat et al., 2011). Lowering at rates of 30–35 m/yr (Levinsen et al., 2013), JI has the potential to influence sea level rise more than any other single feature in the Northern Hemisphere.

A recent GRACE study by Velicogna and Wahr (2013) shows that using Release 5.0 (RL05) GRACE fields for January 2003 through November 2012, a mass change of  $-258 \pm 41$  Gt/y for Greenland is found, and a loss that migrated clockwise around the ice sheet margin to progressively affect the entire periphery. Comparison of different studies for recent mass loss in Greenland (Svendsen et al., 2013) shows local disagreement between the data products. However, all models agree that the acceleration in mass loss is largely confined to the west-northwestern part of Greenland.

Establishing the presence of an acceleration on the order of magnitude found in the Greenland Ice Sheet re-

quires more than 5 years of data, and we find that the GRACE time series available are now long enough to establish the presence of such an acceleration. Maximally four years of reprocessed GOCE gradient observations will be available by mid-2014, which may add the supplement GRACE derived solution for mass changes.

The GRACE satellites are 450 km above the Earth's surface, which makes them relatively insensitive to short-scale terms in the gravity field. This means that the processing centers remove short-scale terms by truncating their solutions to a finite set of low-degree harmonics 60 for Release 5.0 (RL05) fields calculated by CSR (the Center for Space Research at the University of Texas) and 90 for solution calculated by GFZ (GeoForschungsZentrum in Potsdam), see Velicogna and Wahr (2013). This results in spatial resolution of approximately 330 km. Gradient data from the GOCE satellite mission, having the spatial resolution of approximately 100km, may improve the resolution of observed ice mass changes.

The full range of possibilities for the use of GOCE gradients are still not fully recognized. Even though ocean studies already benefit from the GOCE gradients (Herceg, 2012), their contribution to the solid Earth applications is still to follow.

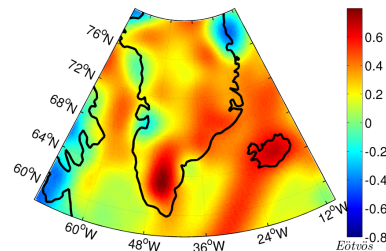
The aim of this study is to present the methodology for using GOCE gradients to possibly extract the signal that corresponds to the signal of change in *JI* ice mass. In order to present GOCE capabilities of detecting ice mass change by using second order derivatives of gravitational potential observed by GOCE, the used time interval spans from November 2009 to June 2010.

## 2 GOCE $T_{zz}$ gravity gradients

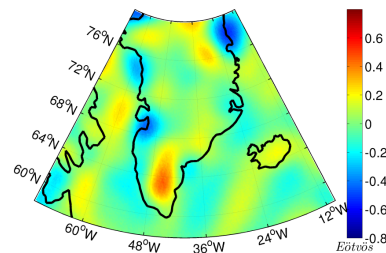
As the result of the processing of satellite data, the GOCE mission provides many products. One of these products are gravity gradients given in the Terrestrial Reference Frame (TRF). The available GOCE level 2 TRF data products, which are offered to the GOCE user community, are packed in monthly and sub-monthly packages (Table 1) in the Earth Explorers File Format Standards (EEF) format (Floberghagen et al., 2010).

The GOCE gradient dataset contains 6 elements of full gravity gradient matrix with associated errors. In this study only  $T_{zz}$  GOCE gradients were used, since adding the  $T_{yy}$  GOCE gradients component when using the Least-Squares Collocation (LSC) method only provides marginal improvements to the results obtained when solely using  $T_{zz}$  (Tscherning and Arabelos, 2011).

In order to produce the gravity anomaly residuals, the long wavelength part of the gravity field must be therefore subtracted. In this study, the gravity field contribution up to harmonic degree and order 36 is subtracted from the GOCE gradients (Fig. 1).



(a) GOCE  $T_{zz}$  gradients.



(b) GOCE  $T_{zz}$  gradient anomalies when the contribution up to degree 36 is subtracted.

**Fig. 1.** Reprocessed GOCE  $T_{zz}$  gradients (a) and GOCE  $T_{zz}$  gradient anomalies (b) when the contribution from Earth's Gravitational Model 2008 (EGM2008) up to spherical harmonic degree and order 36 is subtracted. The dataset consists of data from November 2009 to June 2010. The given units are *Eötvös*.

GOCE  $T_{zz}$  gravity gradients in the Greenland region range between  $-0.4$  and  $+1.0$  *Eötvös*. Strong gravity gradients (around  $+1.0$  *Eötvös*) are present in the southern part of Greenland and along the central-eastern parts of the ice sheet (Fig. 1a). This indicates excess of masses compared to the reference model (gradients computed from normal the potential of the reference ellipsoid), an excess, whose source may come from the Earth's interior or from the Greenland Ice Sheet. Near-zero and weak positive  $T_{zz}$  gravity gradients (up to  $0.2$  *Eötvös*) are present in most parts of Greenland, while weak negative gravity gradients are only present in the *JI* region.

Removing the contribution up to spherical harmonic degree and order 36 subtracts the contribution of the gravity field signal with wavelengths longer than 500km. This

**Table 1.** GOCE TRF gradient data packages and related time interval covered.

Package	Used GOCE TRF datasets
1	GO_CONS_EGG_TRF_2_20091101T000000_20091130T235959_0100.EDF
2	GO_CONS_EGG_TRF_2_20091201T000000_20091231T235959_0100.EDF
3	GO_CONS_EGG_TRF_2_20100101T000000_20100111T235959_0100.EDF
4	GO_CONS_EGG_TRF_2_20100112T000000_20100131T235959_0100.EDF
5	GO_CONS_EGG_TRF_2_20100201T000000_20100212T235959_0100.EDF
6	GO_CONS_EGG_TRF_2_20100303T000000_20100304T235959_0100.EDF
7	GO_CONS_EGG_TRF_2_20100306T000000_20100319T235959_0100.EDF
8	GO_CONS_EGG_TRF_2_20100325T000000_20100331T235959_0100.EDF
9	GO_CONS_EGG_TRF_2_20100401T000000_20100430T235959_0100.EDF
10	GO_CONS_EGG_TRF_2_20100501T000000_20100506T235959_0100.EDF
11	GO_CONS_EGG_TRF_2_20100507T000000_20100531T235959_0100.EDF
12	GO_CONS_EGG_TRF_2_20100601T000000_20100630T235959_0100.EDF

allows calculations in local regions, since the results are not contaminated by the gravity field outside of the study area. For the truncation of the GOCE gravity gradients, the EGM2008 global geopotential model is used (Fig. 1b and Fig. 2). The EGM2008 up to degree 2190 has been developed by Pavlis et al. (2012), and it incorporates shipborne, airborne, and satellite altimetry derived gravity anomalies. It also has benefited from the Gravity Recovery and Climate Experiment (GRACE) based satellite solutions.

Truncation of the GOCE  $T_{zz}$  gradients, yields the corresponding gradient anomalies (Fig. 1b for combined months and Fig. 2 for monthly solutions). Calculated gradient anomalies for the Greenland region range between  $-0.4$  and  $+0.4$  Eötvös, which indicates a gradient signal of around  $+0.4$  Eötvös, which was removed in truncation. Comparing the full-spectrum GOCE  $T_{zz}$  gradients and the truncated result, it is clear that truncation has the strongest effect in the southern part of Greenland as well as along the central-eastern coast, *i.e.* places where the full spectrum gradient signal was strongest.

Monthly solutions for the GOCE  $T_{zz}$  gradient anomaly show a very similar gravity signal (Fig. 2). However, some months have data gaps that leaves the part of Greenland without data coverage (Fig. 2d for February and Fig. 2e for March).

The spatial resolution of GOCE data is around 100 km (this can be observed on Fig. 2), while that of GRACE barely exceeds 330 km. The high spatial resolution of GOCE observations may lead to more detailed mapping of ice mass changes.

High  $T_{zz}$  gradient anomalies (approximately  $+0.4$  Eötvös) are still present in the southern part of Greenland (Fig. 2), while the area along the central-eastern coast shows near-zero and weak negative gradient anomalies. Very significant is that strong negative gradient anomalies are present in the area near two of Greenland's largest out-

let glaciers, *i.e.* JI and the Helheim glaciers. This may reflect low-density masses in these regions or rather a lack of masses compared to the reference model and the removed contribution up to spherical harmonic degree and order 36.

### 3 Prediction of the gravity anomaly using GOCE $T_{zz}$ gradients

For regional gravity anomaly prediction in this study, two methods are used, one of them being LSC (developed by C. C. Tscherning, 1974) and the other the Reduced Point Mass (RPM) method (developed by Herceg, 2012). Both methods show good agreement in prediction of the gravity anomaly residuals, which will be demonstrated in the comparison section. Compared to the LSC method, the RPM method needs less time for calculation since the number of equations needed to be solved in LSC depends on the number of observations. With RPM, the number of equations is dependent on the number of gridded point masses.

#### 3.1 The Least-Squares Collocation method

LSC enables the use of many types of observables (Krarup, 1969) for the estimation of gravity field quantities and their errors.

The basic observation equation for LSC is

$$y_i = L_i T_{LSC} + e_i \quad (1)$$

where  $e_i$  is the error contribution. The estimate of  $T_{LSC}$  is obtained by

$$\tilde{T}_{LSC}(P) = \{C_{Pi}\}^T \tilde{C}^{-1} \{y\} \quad (2)$$

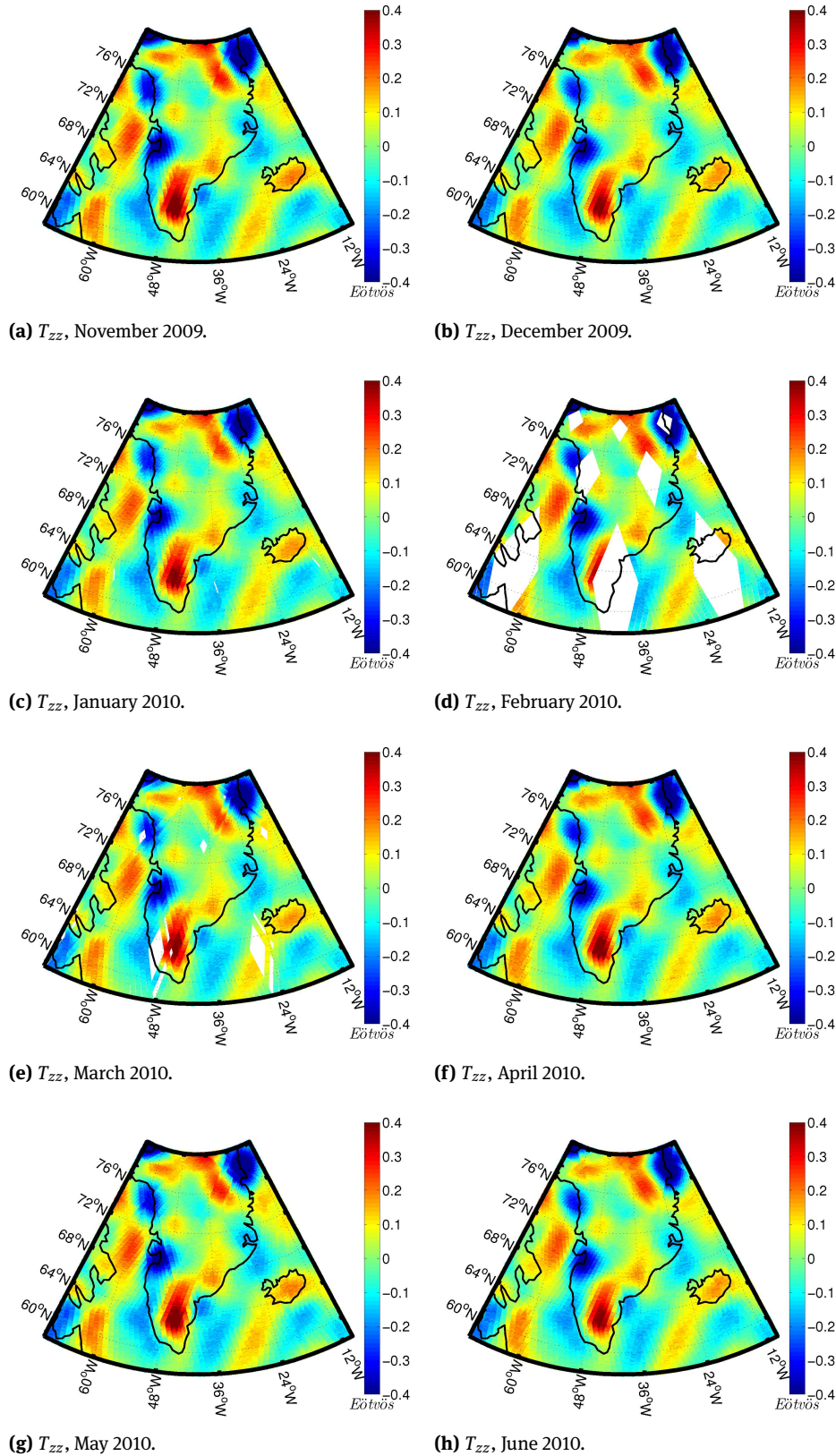


**Fig. 2.** Monthly solutions for GOCE  $T_{zz}$  gradients when the contribution from the global model EGM2008 up to spherical harmonic degree and order 36 is subtracted. The given units are Eötvös.

where  $\tilde{T}_{LSC}(P)$  is the estimated quantity,  $C_{p_i}$  is a vector which contains the covariance values between the estimated quantity and observations, and  $\tilde{C} = \{C_{ij} + \sigma_{ij}\}$ , where  $C_{ij}$  and  $\sigma_{ij}$  are matrices containing the signal covariance and the error covariance values, respectively, between the observations  $y$  (Tscherning, 1976).

Analytic covariance models are used in LSC for regional applications. The optimal covariance function for a region is selected by fitting an analytic model to empirically determined values. Here, the empirically determined values are obtained by using the program *EMPCOV* (Forsberg and Tscherning, 2008) on data in a certain region.

To fit empirical covariance functions to isotropic analytic models, the Fortran program *covfit.f* from *GRAVSOFIT* package was used (Knudsen, 1987). The parameters obtained by fitting the covariance function were used in the collocation prediction method as well as the reduced point mass prediction.

### 3.2 The Reduced Point Mass (RPM) method

There are different implementations of the point mass methodology for local gravity field determination, and they are already described in many publications, see e.g. Herceg (2012), Tscherning et al. (2010), Vermeer (1992), Vermeer (1982), Sjogren et al. (1971).

Point-mass functions are harmonic functions, which may be used to represent  $T$  either globally or locally, and they can be expressed by either closed expressions or as sums of Legendre series. In both cases at least the two first terms must be removed since they are not present in  $T$ , i.e. zero-degree ( $l=0$ ) harmonic terms cancel each other out and the first degree harmonics ( $l=1$ ) are equal to zero since the origin of the coordinate system is chosen to coincide with the geocentre. For local applications the effect of a global gravity model is generally removed and later on restored.

The anomalous gravity field,  $T$ , at computational point  $Q$  is modeled by a set of base functions, each obtained as the anomalous gravity potential from each point mass  $m_i$  located at the position  $P_i$  on the Bjerhammer sphere with radius  $R_M$  estimated with using LSC method. This radius of point masses,  $R_M$ , is smaller than that of the Earth,  $R_E$ .

$$T(Q) = \sum_i T_i(Q) \quad \text{and} \quad T_i(Q) = V_i(Q) - U_i(Q) \quad (3)$$

where  $V$  and  $U$  are the Earth's gravity and normal potential, respectively.

Normally, a gravitational potential function is related to the position in terms of spherical coordinates  $(\phi, \lambda, r)$ .

If the potential is considered,  $V = V(\lambda, \phi, r)$ , the gradient of  $V$  is defined in the geocentric  $(x, y, z)$  or local rectangular  $(\eta, \xi, \zeta)$  Cartesian coordinate system in the normalized basis as (Herceg, 2012):

$$\nabla V = \frac{1}{r \cos \phi} V_\lambda \hat{e}_1 + \frac{1}{r} V_\phi \hat{e}_2 + V_r \hat{e}_3 \quad (4)$$

Here the local coordinate system is described by the basis  $e_p$  with vectors in triad  $(e_1, e_2, e_3)$ , which are not unit vectors.

When using point masses, the closed expression for the vertical second order derivatives of the potential in the  $(\eta, \xi, \zeta)$  system are given as (Herceg, 2012):

$$V_{\zeta\zeta} = \frac{\partial^2 V}{\partial r_p^2} = -\frac{1}{l^3} + 3 \frac{(r_p - r_q t)^2}{l^5} \quad (5)$$

where  $t$  is the cosine of the spherical distance  $\psi$  between two points ( $P$  and  $Q$ ), and the partial differential equation of second order satisfies the *Laplacian differential equation*,  $\Delta V = 0$ .

Reduced gravity potential,  $V_R$  is represented through reduced point masses, which are point mass functions where the first  $n$  harmonics have been removed. For the expressions of gravity gradients, when using reduced point masses, the derivative of the sum of a finite Legendre series is used:

$$S = \sum_{m=0}^n a_l s^{m+1} P_m(t) \quad (6)$$

Here,  $m$  is degree of the Legendre polynomial  $P$ ,  $s$  contains the parameters or the anomaly degree variance model,  $t$  is the cosine of the spherical distance  $\psi$  between two points, and  $a_l$  represents the multiplication factor, which depends on the derivative with respect to  $r_Q$ . For these, we have series expansions similar to Eq. (6) where the terms for the first derivative are multiplied with  $a_1 = -(i+1)/r_Q$  and for the second derivative with  $a_2 = (i+1)(i+2)/r_Q^2$ .

The derivative of the sum of a finite Legendre series can be computed easily using a recursion algorithm (Tscherning and Rapp, 1974). For

$$e_l = \frac{2l+1}{l+1} s \quad (7)$$

$$f_{l+1} = -\frac{l+1}{l+2} s^2$$

and

$$b_l = e_l t b_{l+1} + f_{l+1} b_{l+2} + a_l \quad (8)$$

with  $b_{n+1} = b_{n+2} = 0$ , we have

$$S = b_0 s \quad (9)$$

The derivatives of  $S$  with respect to  $t$  are then computed by a recursion algorithm obtained by Eq. (8) (Tscherning, 1976):

$$b_l^1 = e_l (b_{l+1}^1 + t b_{l+1}^1) + f_{l+1} b_{l+2}^1 \quad (10)$$

$$b_l^2 = e_l (2b_{l+1}^2 + t b_{l+1}^2) + f_{l+1} b_{l+2}^2 \quad (11)$$

Thus, the expression for the vertical second order derivative of the gravitational potential in the  $\zeta$  direction is (Herceg, 2012):

$$V_{\zeta\zeta R} = \frac{\partial^2 V_R}{\partial r_P^2} \quad (12)$$

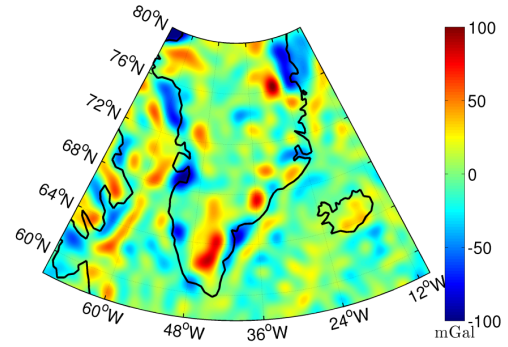
Here, the partial derivatives of the spherical distance  $\psi$  with respect to the latitude and longitude are expressed through  $t$ , as in Herceg (2012).

This approach is able to tailor the algorithm for point mass depth and grid spacing relations. The method provides the calculation of both full and reduced gravity field quantities using either full or reduced point masses, respectively. Gravity anomaly determination by means of the reduced point masses can be used as an alternative method to the conventional ones for local gravity field determination.

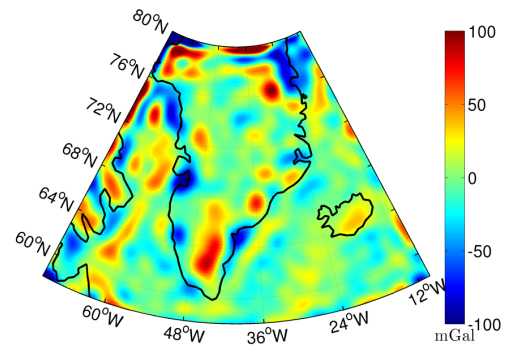
The prediction of reduced point masses cannot be used for the estimation of absolute masses in local regions, but may supplement the determination of relative mass changes. The gravity gradient anomalies can then be used in the RPM method for the calculation of ice mass change in a given time interval.

### 3.3 Comparison of the LSC and RPM results

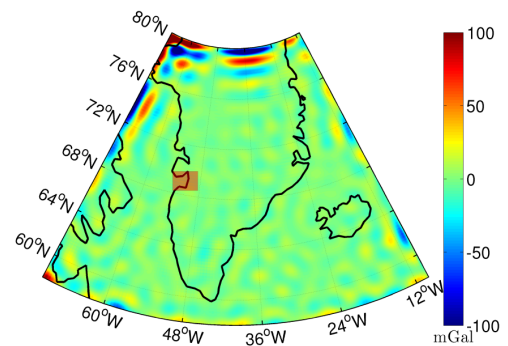
The predicted gravity anomaly residuals found using collocation have a standard deviation (std) of 25.94 mGal at the surface, while the std of the RMP results is 35.32 mGal. Both methods presented here show good agreement in the prediction of gravity anomaly residuals (Fig. 3). Strong gravity anomaly signals are present mostly in the southern and north-eastern parts, where it exceeds 100 mGal. Negative gravity anomaly residuals are present mostly near



(a) Predicted gravity anomaly residual for December 2009, using collocation.



(b) Predicted gravity anomaly residual for December 2009, using RPM.



(c) Difference

**Fig. 3.** Comparison of predicted gravity anomaly residuals found using LSC (a) and the RPM (b) respectively. Area of Jakobshavn Isbræ glacier is outlined red in the difference (c). The observations used are acquired in December 2009.

Jl and the Helheim glacier as well as in the northwestern part.

In the following section, the RPM method will be used for determination of the gravity anomaly change occurring from November 2009 - June 2010 and corresponding relative mass changes in Greenland.

The results of the gravity anomaly changes will then be compared to the gravity anomaly changes resulting from changes in ice mass topography calculated from a Digital Elevation Model (DEM) for the JI drainage basin.

The method and data used for the prediction of gravity anomaly changes by changes in ice mass topography is described in the following section.

## 4 Prediction of mass changes using GOCE $T_{zz}$ gradients and the RPM method - Jakobshavn Isbræ drainage basin

Even though an observed mass loss in Greenland has been substantial over the last decade (Fig. 4), the largest lowering of the ice surface is observed over the largest outlet glacier on Greenland's west coast, namely Jakobshavn Isbræ (JI) (Fig. 5). This glacier loses the most mass and has doubled its contribution to global sea level rise over the last decade (Howat et al. (2011), Khan et al. (2010), Joughin et al. (2014)).

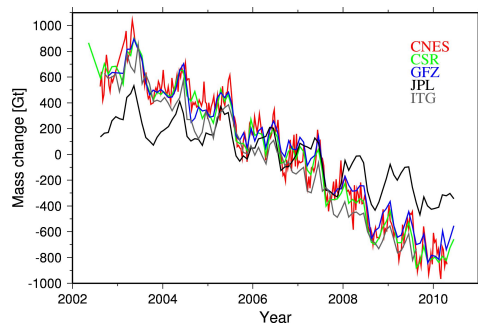


**Fig. 4.** Observed Greenland mass change over the last decade. Time series of GrlS (Greenland Ice Sheet) from GFZ (GeoForschungs Zentrum), CSR (Center for Space Research), JPL (Jet Propulsion Laboratory), CNES (Centre National d'Etudes Spatiales) and ITG (The Institute of Theoretical Geodesy). Figure credit: Sørensen (2010).

Greenland mass loss observed using gravity gradients may supplement the methods for observing surface elevation changes in determining whether the ice surface is thinning or thickening. In order to analyze the GOCE grav-

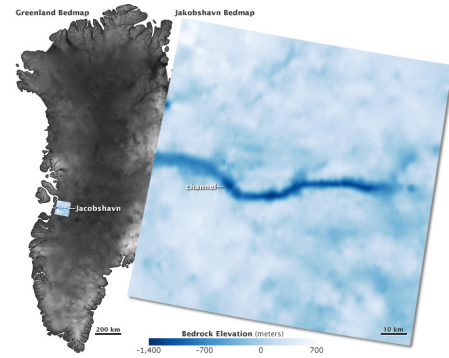


**Fig. 5.** Greenland and Jakobshavn Isbræ bed map elevations. Figure credit: NASA Earth Observatory.

ity gradient sensitivity on ice mass changes, a study on JI drainage basin ice mass change will be presented.

Gravity anomalies arising from changes in the surface topography can be approximated using a simple Bouguer correction. When applying it, the masses are approximated by a flat, homogeneous and infinite plate, a so-called Bouguer plate, which has the density  $\rho$  and the height  $h$  (Sansó et al., 2013):

$$\delta g_B = 2\pi G\rho h = 0.04192\rho h \quad (13)$$

If we assume that the surface consists of only ice and that this has a density of  $0.92 \frac{g}{cm^3}$ , the Bouguer correction can be expressed as

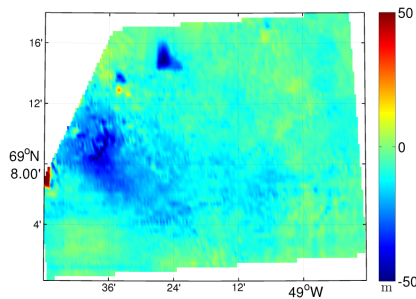
$$\delta g_B = 0.0386h \quad [mGal] \quad (14)$$

The gravity anomaly changes (Fig. 6b) resulting from changes in ice mass topography (Fig. 6a), calculated using Eq. (14), show variations of  $\pm 2$  mGal. This corresponds to an ice mass topography change of  $\pm 50$  m.

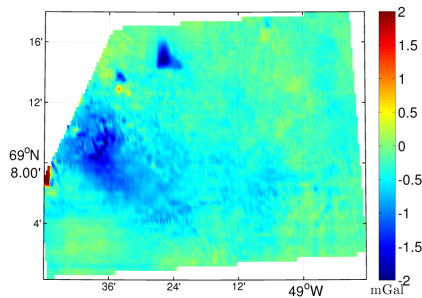
Here, the JI drainage basin is studied using Digital Elevation Models (DEMs). The spatial resolution of the data is  $0.001^\circ$ , i.e. approximately 110 m in the north-south direction and around 55 m in the west-east direction (Levensen et al., 2013). These were developed by co-registering stereoscopic imagery from SPOT-5 to airborne and spaceborne laser data agreeing in time and space. The latter data are acquired with the National Aeronautics and Space Administration (NASA) laser scanner on-board the Airborne Topographic Mapper (ATM), and the Geoscience Laser Altimeter System (GLAS) on-board the Ice, Cloud and land Elevation Satellite (ICESat). The imagery has a high spatial resolution of approximately  $40 \times 40$  m however elevation errors on the order of 10 – 15 m; the laser data has errors one order of magnitude smaller, however are constrained to satellite orbits and flight paths. Thus, by minimizing planimetric and elevation-dependent biases in be-



tween the two datasets, any offsets between them were reduced, and high-resolution DEMs with low elevation errors were produced (Levinsen et al., 2013).



(a) Surface elevation changes derived from a combination of airborne and spaceborne laser data with stereoscopic imagery.



(b) Gravity changes.

**Fig. 6.** Surface elevation changes over JI drainage basin (a), and the corresponding gravity changes (b) calculated using Eq. (14). The observation period is from 04.08.2007 to 02.08.2008. The area shown corresponds to the region of Jakobshavn Isbræ glacier shown in Fig. 5.

A similar calculation is made with the *Gravsoft TC* program (Tscherning et al., 1992). This can calculate the direct topographic effects of all masses above a reference level, assuming the density to be constant. The computation is based on two digital elevation models, a detailed and a coarse, which are used in the inner and outer zones, respectively. The two grids are assumed to have common boundaries, which is the case if the coarse grid has been constructed from the detailed grid by averaging. The integration of the terrain effects is performed using the formulas for the gravitational effects of a homogeneous rectangular prism. Depending on the geometry and accuracy, either exact formulas, spherical harmonic expansion, or a centered point mass approximation is used. The effect of

the ice topography change on the gravity anomaly is calculated using the *TC* program (Fig. 7).

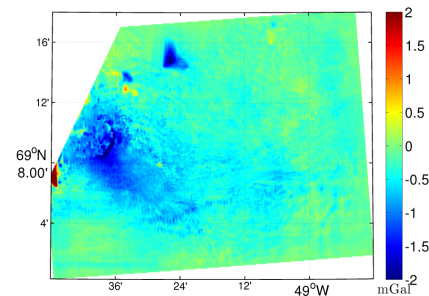


**Fig. 7.** Gravity changes calculated using the *Gravsoft TC* program from 04.08.2007 to 02.08.2008. The area shown corresponds to the region of Jakobshavn Isbræ glacier shown in Fig. 5.

The results from using the Bouguer correction (Fig. 6b) and the *TC* program (Fig. 7), respectively, show a very good agreement in the prediction of gravity anomaly changes from a change in topography. However, more details in the gravity anomaly changes are present when using *TC*. The maximum gravity changes observed by the surface of the JI drainage basin range from 2 – 4 mGal for the period considered. The error when estimating gravity anomalies from GOCE gradient data using only the  $T_{ZZ}$  gradient component is 11 mGal when the associated data error is 20 mE.

The gravity anomaly change occurring from November 2009 - June 2010 shows variations of  $\pm 30$  mGal when using GOCE  $T_{ZZ}$  gradients (Fig. 8). However, the small signal in the results is probably contaminated by the error in the GOCE  $T_{ZZ}$  gradient dataset.

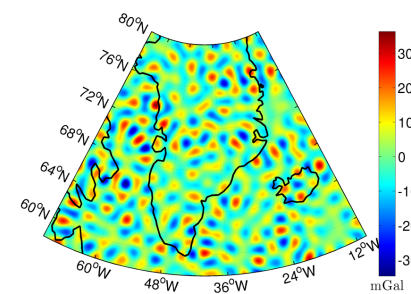


**Fig. 8.** Gravity anomaly change between November 2009 and June 2010 observed using GOCE  $T_{ZZ}$  gradients.

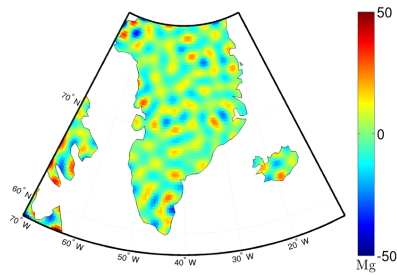


**Fig. 9.** Ice sheet residual mass change between November 2009 and June 2010 observed using GOCE  $T_{ZZ}$  gradients.

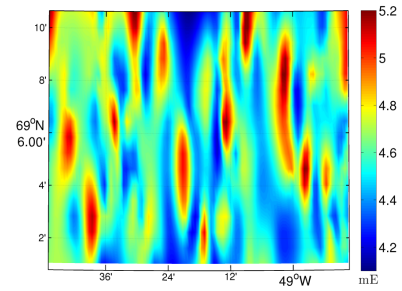
The corresponding ice sheet residual mass change (Fig. 9) shows a variation of  $\pm 50$  Mg. The largest changes occur in the center of the ice sheet, and not around the ice margin, thereby ignoring the rapidly changing outlet glaciers.

To further inspect the sensitivity of GOCE  $T_{zz}$  gradients on ice cover thickness, the *TC* program was used to compute the topographic effects of the gravity gradient. The gravity gradient topographic effects were calculated for two time intervals, 04.08.2007 (Fig. 10a) and 02.08.2008 (Fig. 10b). The maximum vertical gradient change at satellite altitude for the Jakobshavn area from August 2007 - August 2008 is 0.2 mE (Fig. 10c).

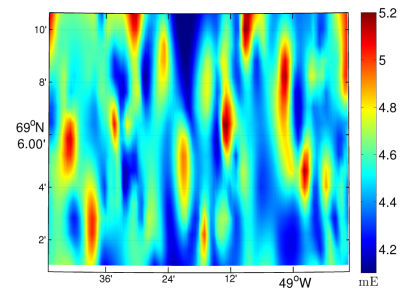
The gradients observed with GOCE have a minimum error of 3 mE for the along-track component, and a combination of all four available components could potentially lower this to 1 mE. Furthermore, we would need a longer period of GOCE  $T_{zz}$  gradient observations; a qualified guess is five years in order to observe this small signal. We expect maximally four years of observations to be available by mid-2014. Furthermore, starting from August 2012, the GOCE mission control team initiated the lowering of GOCE at a rate of approximately 300 meters per day. The objective is to lower the satellite from its nominal orbit of 255 km to a recommended height of 235. This will increase the accuracy and spatial resolution of the GOCE measurements, which may lead to the accuracy necessary to observe ice mass changes by the methods presented here.

## 5 Conclusions

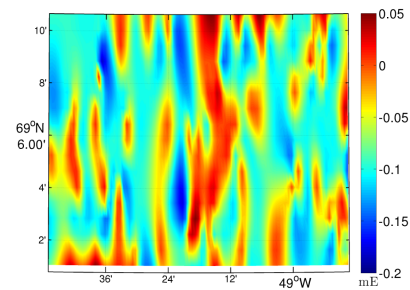
The estimated gravity anomalies on the ground are very similar for the two methods used. However, both methods are affected by the lack of several tracks in the monthly datasets. An idea for the calculation of the quantities year



**(a)**  $T_{zz}$  gravity gradient on 04.08.2007.



**(b)**  $T_{zz}$  gravity gradient on 02.08.2008.



**(c)**  $T_{zz}$  gravity gradient change between 04.08.2007 and 02.08.2008.

**Fig. 10.**  $T_{zz}$  gravity gradients at satellite altitude for the two different time intervals, (a) and (b), and the change between the two (c) due to the mass change. The given units are *Eötvös*.

by year and season by season was also tested, however did not lead to a higher signal in ice mass change.

The maximum vertical gradient change at satellite altitude for the Jakobshavn Isbræ drainage basin area from August 2007 - August 2008 is 0.2 mE. The gradients observed by GOCE have a minimum error of 3 mE for the along-track component, and a combination of all four available components could potentially lower this error to 1 mE. Consequently, a 5-year observation period is necessary in order to observe such a small signal. Four years of

reprocessed GOCE observations will be available by mid 2014.

The maximum gravity changes at the ground are between 2 and 4 mGal for the period considered. The gravity anomaly estimation error arising from the GOCE gradient data using only  $T_{zz}$  with an associated error of 20 mE is 11 mGal. Using more gradient components in the Gradiometer Reference Frame (GRF) would certainly reduce this error, presumably to 5 – 6 mGal. Thus, change detection may be made possible over two to three year periods.

There is hope for future GOCE data acquisitions to be able to further our understanding of mass changes using gravity gradients and gradient anomalies. We expect maximally four years of GOCE gradient observations to be available at the middle of 2014. Furthermore, lowering of the GOCE satellite down to an orbit of 235 km will increase the accuracy and spatial resolution of the measurements. This may then lead to the accuracy needed in order to observe ice mass changes using the GOCE gravity gradients. A new GOCE-type mission, with improved accuracy, will undoubtedly provide the possibility to detect areas of mass gain or losses over short time periods.

## References

- Floberghagen, R., Muzi, D., De la Feld, F., B., W., Rummel, R., Gruber, T., and Van Hees, R. (2010). GOCE High Level Processing Facility: GOCE Level 2 Product Data Handbook.
- Forsberg, R. and Tscherning, C. C. (2008). *An overview manual for the GRAVSOFT, Geodetic Gravity Field Modelling Programs*, 2 edition.
- Herceg, M. (2012). *GOCE data for Ocean Modelling*. PhD thesis, DTU Space, National Space Institute, Technical University of Denmark.
- Howat, I. M., Ahn, Y., Joughin, I., Van den Broeke, M. R., and Lenaerts, J. T. M. and, S. B. (2011). Mass balance of greenland's three largest outlet glaciers, 2000–2010. *Geophysical Research Letters*, 38 (12).
- Joughin, I., Smith, B., Howat, I. M., Scambos, T., and Moon, T. (2010). Greenland flow variability from ice-sheet-wide velocity mapping. *Journal of Glaciology*, 56:415–430.
- Joughin, I., Smith, B. E., Shean, D. E., and Floricioiu, D., (2014). Brief Communication: Further summer speedup of Jakobshavn Isbræ, *The Cryosphere*, 8, 209-214, doi:10.5194/tc-8-209-2014.
- Khan, S. A., Wahr, J., Bevis, M., Velicogna, I., and Kendrick, E. (2010). Spread of ice mass loss into northwest greenland observed by grace and gps. *Geophysical Research Letters*, 37(6).
- Knudsen, P. (1987). Estimation and modelling of the local empirical covariance function using gravity and satellite altimeter data. *Bulletin Geodesique*, vol. 61:pp. 145–160.
- Krabill, W., Hanna, E., Huybrechts, P., Abdalati, W., Cappelen, J., Csatho, B., Frederick, E., Manizade, S., Martin, C., Sonntag, J., Swift, R., Thomas, R., and Yungel, J. (2004). Greenland ice sheet: Increased coastal thinning. *Geophysical Research Letters*, 31(24):n/a–n/a.
- Krarpup, T. (1969). A Contribution to the Mathematical Foundation of Physical Geodesy. *Meddelelse no. 44, Geodaetisk Institut, Koebenhavn*.
- Levinsen, J. F., Howat, I. M., and Tscherning, C. C. (2013). Improving maps of ice sheet surface elevation change using combined laser altimeter and stereoscopic elevation model data. *Journal of Glaciology*, 59, no. 215.
- Pavlis, E., Holmes, S., Kenyon, S., and Factor, J. (2012). The development and evaluation of the Earth Gravitational Model 2008 (EGM2008). *Journal of Geophysics Research*, 117:38.
- Sansó, F., Sideris, M. G., Tscherning, C., Pavlis, N., Tziavos, I., Andersen, O., and Fotopoulos, G. (2013). *Geoid Determination - Theory and Methods*, volume 110 of *Lecture Notes in Earth System Sciences*. Springer Berlin Heidelberg.
- Sjogren, W., Muller, P., Gottlieb, P., Wong, L., Buechler, G., Downs, W., and Prislín, R. (1971). Lunar surface mass distribution from dynamical point-mass solution. *The moon*, 2:338–353.
- Sørensen, L. S. (2010). *Changes of the Greenland ice sheet - derived from ICESat and GRACE data*. PhD thesis, DTU Space.
- Svendsen, P., Andersen, O., and Nielsen, A. (2013). Acceleration of the greenland ice sheet mass loss as observed by grace: Confidence and sensitivity. *Earth and Planetary Science Letters*, 364(0):24 – 29.
- Tscherning, C., Forsberg, R., and Knudsen, P. (1992.). GRAVSOFT - A System for Geodetic Gravity Field Modelling. *Proc. 1. Continental Workshop on the Geoid in Europe, Research Institute of Geodesy, Topography and Cartography, Prague*, pages 327–334.
- Tscherning, C. C. (1976). Covariance Expressions for Second and Lower Order Derivatives of the Anomalous Potential. *Reports of the Department of Geodetic Science No. 225, The Ohio State University, Columbus, Ohio*.
- Tscherning, C. C. and Arabelos, D. (2011). Gravity anomaly and gradient recovery from GOCE gradient data using LSC and comparisons with known ground data. *Proceedings 4th International GOCE user workshop, ESA Publications Division, Noordwijk, The Netherlands*.
- Tscherning, C. C. and Rapp, R. H. (1974). Closed Covariance Expressions for Gravity Anomalies, Geoid Undulations, and Deflections of the Vertical Implied by Anomaly Degree-Variance Models. *Reports of the Department of Geodetic Science No. 208, The Ohio State University, Columbus, Ohio*.
- Tscherning, C. C., Veichert, M., and Herceg, M. (2010). Reduced point mass or multipole base functions. *Contadakis ME, Katsikis C, Spatalas S, Tokmakidis K, Tziavos IN (eds), The Apople of the Knowledge, Honorary Volume to Emeritus Professor Demetrius Arabelos, Ziti Editions, ISBN: 978-960-243-674-5, pages 282–289*.
- Velicogna, I. and Wahr, J. (2005). Greenland mass balance from grace. *Geophysical Research Letters*, 32(18).
- Velicogna, I. and Wahr, J. (2013). Time-variable gravity observations of ice sheet mass balance: Precision and limitations of the grace satellite data. *Geophysical Research Letters*, 40(12):3055–3063.
- Vermeer, M. (1982). The use of mass point models for describing the Finnish gravity field. *Proceedings, 9th Meeting Nordic Geodetic Commission, Gaevle, Sweden*.

Vermeer, M. (1992). Geoid determination with mass point frequency domain inversion in the Mediterranean. *Mare Nostrum 2, GEOMED report, Madrid*, pages 109–119.

Received August, 13 2013; accepted January, 20 2014.